A MODIFIED DISCRETE MODEL IN THE NONLINEAR FINITE ELEMENT ANALYSIS OF PRESTRESSED AND REINFORCED CONCRETE STRUCTURES

Mohammed Arafa[1] and Gerhard Mehlhorn[2]
University of Kassel, Department of Structural Concrete,
Kurt Wolters Str. 3, D-34109 Kassel, Germany.

SUMMARY

A special discrete and smeared representation of reinforcement to be used in nonlinear finite element analysis of prestressed and reinforced concrete structures is presented. In this technique the main reinforcing bars of arbitrary type and location can be represented using a discrete model independent of the concrete finite element mesh. Whilst the secondary reinforcement and/or stirrups are represented by a smeared model. Lagrange and Serendipity quadratic and cubic isoparametric elements with movable side and interior nodes are used. A contact element with different bond conditions is used to model the bond behaviour between concrete and steel. The frictional force in prestressed tendon is easy to represent.

Keywords: discrete model, FEA, prestressing

1. INTRODUCTION

The discrete modelling of steel reinforcement is the first approach used in the finite element analysis of reinforced concrete structures. It was originally suggested by [NGO/SCORDELIS 67] in their earliest published application.

In the discrete model the reinforcing bars are generally modelled as separate elements, commonly truss or cable elements. The location of the steel elements is determined by the layout of the reinforcement. Consequently, the boundaries of the concrete elements have to follow the reinforcing bar. The discrete representation of reinforcement is the only way of accounting for bond slip and dowel action directly. The main disadvantage is that the finite element mesh patterns are restricted by the location of reinforcement and consequently the increase of the number of concrete elements and Degrees Of Freedoms (DOFs) [HOFSTETTER/MANG 95].

In order to allow independent choice of concrete mesh, [EL-MEZAINI/CITIPITOGLU 91] used a Serendipity isoparametric element with movable side nodes. In their presentation a line as two node truss elements is used to represent the steel, although a quadratic or cubic isoparametric element for concrete is used. In this way the compatibility between

---

[1] Ph.D. Student
[2] Prof. Dr.-Ing. Dr.-Ing. E.h., Professor in Structural Engineering.

concrete and steel elements cannot be guaranteed. Also the representation of the cable layout is approximated as straight elements.

Embedded models allow an independent choice of concrete mesh. So the same type of elements with the same number of nodes and DOFs are used for both concrete and steel. The disadvantage of this model is that additional DOFs, increase of the computational effort and a special reinforcement element are required.

In the smeared model the reinforcement is characterised by smearing the reinforcing bar to thin layers of mechanically equivalent thickness within a particular concrete element.. However the smeared model only makes sense for uniformly distributed reinforcing bars.

2. NODE MAPPING DISTORTION

Mapping distortion occur when mapping unequally spaced node locations on the sides and interior of the physical element to equally spaced nodes of the parent element. A singular Jacobian matrix is obtained if the edge nodes are moved sufficiently from their normal positions. To allow for flexibility in locating side and interior element nodes, a correction technique for avoiding or minimising this distortion was developed by [CITIPITOGLU/NICOLAS 72] for Serendipity elements and [CELIA & GARY 84] for quadratic two dimensional element. Side nodes are positioned at the same relative distance from corner nodes in both physical and the isoparametric unity element.

The Lagrange shape functions are in principle the shape functions of the Serendipity element extended to the influence of the additional interior nodes.

Therefore all shape functions must fulfil the following constrain conditions:

$$N_{Li}(\boldsymbol{x}_i, \boldsymbol{h}_i) = 1,0 \qquad i = 1, \cdots, n$$
$$N_{Li}(\boldsymbol{x}_j, \boldsymbol{h}_j) = 0,0 \qquad j \neq i, i = 1, \cdots, n \text{ and } j = 1, \cdots, n.$$

(1)

where:

N_{Li}: are the Lagrange shape functions,
n: is number of nodes per element.

The shape functions for the sides and corner nodes are:

$$N_{Li}(\boldsymbol{x}, \boldsymbol{h}) = N_{Si}(\boldsymbol{x}, \boldsymbol{h}) - \sum_{k=1}^{m} N_{Si}(\boldsymbol{x}_k, \boldsymbol{h}_k) N_{Lk}(\boldsymbol{x}, \boldsymbol{h})$$

(2)

N_{Si}: are the Serendipity shape functions
m: is the number of interior node equal to 1 for quadratic and 4 for cubic (see Fig. 1 , 2).

The interior shape function for quadratic element (node 9) is:
$$N_{L9}(\boldsymbol{x}, \boldsymbol{h}) = Q(\boldsymbol{x}, \boldsymbol{x}_9) \cdot Q(\boldsymbol{h}, \boldsymbol{h}_9)$$

(3)

with:

$$Q(\boldsymbol{x},\boldsymbol{x}_k) = \frac{\boldsymbol{x}^2 - 1}{\boldsymbol{x}_k^2 - 1} \qquad (4)$$

If $(\boldsymbol{x}_9 = 0, \boldsymbol{h}_9 = 0)$, the shape functions will be the standard Lagrange shape functions. The interior nodes shape functions for a cubic Lagrange element , is.

$$N_{Lk} = Q(\xi, \xi_k) \cdot Q(\eta, \eta_k) \cdot \varphi_i(\xi, \eta) \qquad (5)$$

Where heir $i = k - 12$

and:

$$\varphi_1(\xi, \eta) = Z_{1,234} + Z_{1,342} + Z_{1,423}$$

$$\varphi_2(\xi, \eta) = Z_{2,134} + Z_{2,341} + Z_{2,421}$$

$$\varphi_3(\xi, \eta) = Z_{3,214} + Z_{3,142} + Z_{3,421}$$

$$\varphi_4(\xi, \eta) = Z_{4,231} + Z_{4,312} + Z_{4,123}$$

(6)

with

$$Z_{i,jkl} = \frac{(\eta - \gamma_j) \cdot (\gamma_k - \gamma_l) \cdot (\xi \cdot \theta_j + \theta_k \cdot \theta_l)}{(\gamma_i - \gamma_j) \cdot (\gamma_k - \gamma_l) \cdot (\theta_i \cdot \theta_j + \theta_k \cdot \theta_l)} \qquad (7)$$

(a)   *(b)*
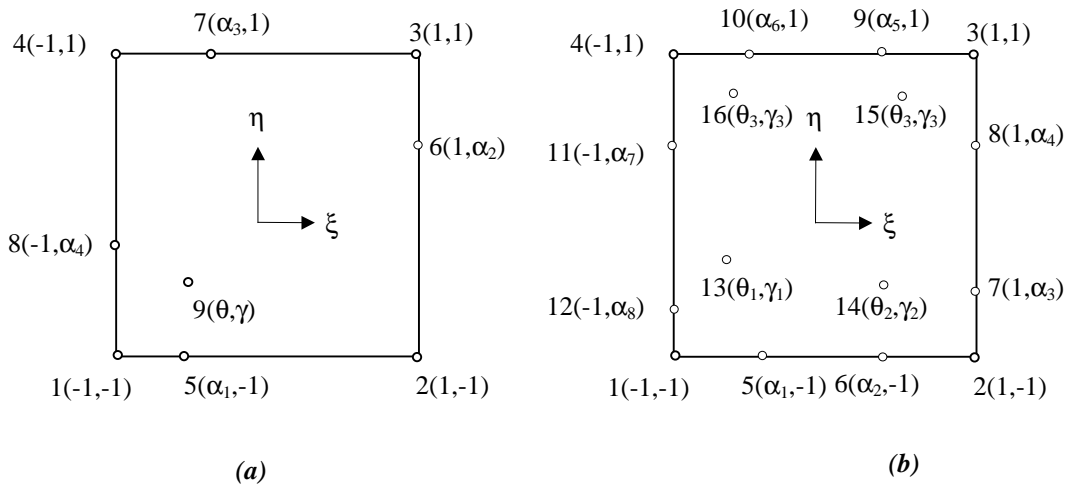
Figure 1 Quadratic and cubic isoparametric element with movable nodes

To demonstrate the effect of node distortion a square plate will be considered as a plane stress element with 9 nodes (see Fig. 2). An elastic linear analysis with the standard and modified shape functions is carried out.

The node Number 5 and 8 have varied positions. The displacements at the node 9 are to be considered. The materials used are E = 10000.0 kN/m^2 ,L=2.0m ,ν=0 and q=30 kN/m.

As seen in (Figs 3a&b) if the nodes 5 or 8 are moved far enough away from their normal positions, a singular Jacobian matrix will be obtained.
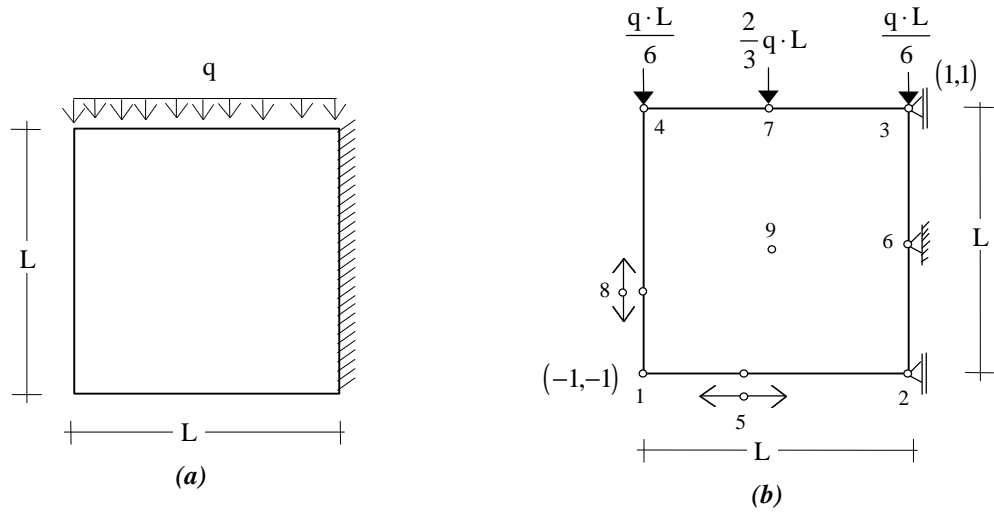
Figure 2 Plate Element and Finite Element Modelling
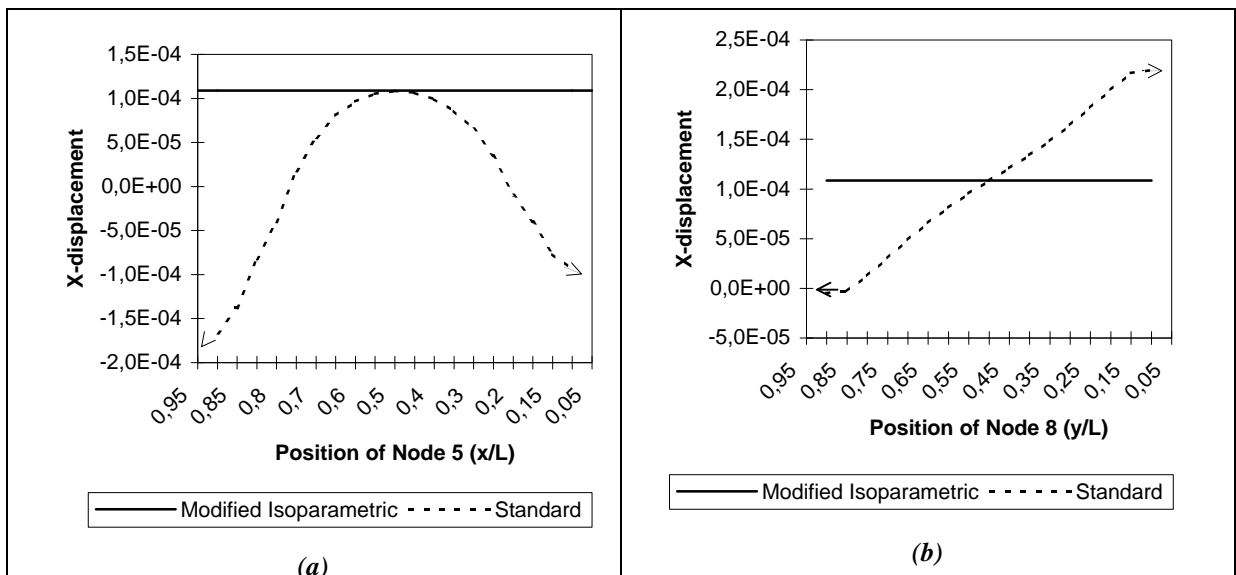
Figure 3 Displacement at Node No. 9 using Modified and Standard Shape Functions

3. MESH GENERATION

As shown in Figure 4 the desired concrete mesh is first selected independently of any reinforcement bars. The secondary reinforcement mesh is set identically to the concrete mesh. Then the concrete side nodes are moved to the points of intersection between the reinforcing bar and the edges of the concrete mesh. The interior node(s), (one node in the case of quadratic element or 2 nodes in the case of the cubic element), are moved to be an interior node(s) of the steel bar. The nodes of the smeared model are moved identically to the concrete model.
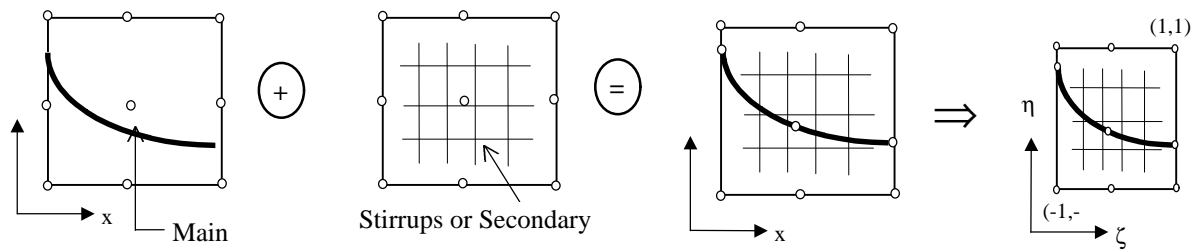
Figure 4 Mesh generation using discrete and smeared element

4. CONCRETE STEEL INTERACTION

Using of the discrete model for representing the main reinforcement has the advantage of representing different material properties more precisely. Different bond conditions at different nodes can be directly and easily represented.

The contact element developed by [KEUSER & MEHLHORN 85] is used to describe the bond behaviour between steel and concrete. In this model the vertical and horizontal relative displacement between concrete and steel in the local coordinates of steel tendon can be considered. This element is an isoparametric element and it has, at the unloaded stage, no physical dimension in the transverse direction. It has two to four double-nodes and uses linear, quadratic or cubic interpolation functions. In the contact interfacing the two elements connected by a contact element have independent element nodes.

In many cases specially in linear analysis the vertical relative displacements are too small compared to the horizontal displacements and can be disregarded. That means that the concrete and steel have the same DOF in local y-direction while they have different DOF in x-direction which are connected to the contact element. The local x-axis is assumed to be parallel to the tangent of the steel tendon.

5. ANALYSIS CONSIDERATION

5.1 Perfect bond analysis

Under service load conditions or in simple linear analysis, it is assumed that the steel tendons are perfectly bonded to the concrete. In this case, there is no slip. This means that the concrete and steel nodes occupying the same location have the same degree of freedom. The stiffness of the steel elements is directly added to the corresponding DOFs in the global stiffness matrix.

5.2 Analysis with no bond

The stiffness matrices of the steel element are calculated in local axis at the node of no bond. The concrete element stiffness matrices are calculated in global axes, then they are transformed to the steel local axes at the common nodes. In local y-direction the concrete and steel have the same DOFs, but in local x-direction concrete and steel have different DOFs., The final displacement at the common points with no bond are obtained in the rotated axes. They can be transformed to the global axes.

5.3 Analysis with bond law

In this case two methods are available:

a) *Considering the vertical and horizontal relative displacement.*

In this case a double node contact element connects the steel and concrete elements. The steel and concrete elements have different DOFs in x- and y-directions see.

b) *Considering only the relative displacement along the steel tendon*

The solution routine is the same as in the no bond case except that the contact element connects the steel and concrete along the steel axis. The steel and concrete have the same DOFs at the common nodes perpendicular to the tendon tangent.

5.4 Representation of the friction force:

The frictional force at the common concrete and steel nodes can be represented as a force along the steel element affected at the corresponding steel's DOF and opposite force affected at the concrete's DOF at the same node.

The frictional force is added to the element force and will be considered in the solution routine (see Fig. 5).
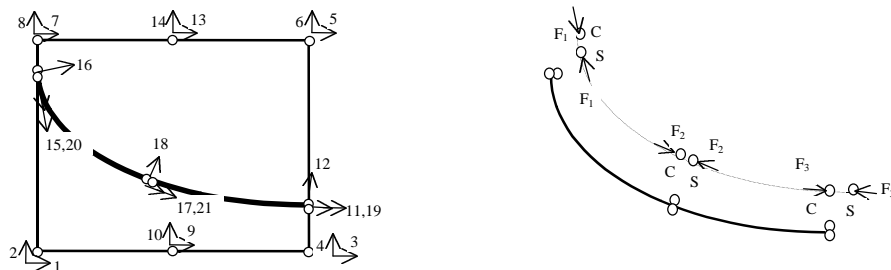
Figure 5 Friction Force Representation

6. NUMERICAL EXAMPLES

The element formulation described above is implemented in the Computer program SEGNID. This program has a nonlinear element library for concrete and steel.

[BRESLER/SCORDELIS 64] have conducted numerous tests on a series of reinforced concrete beams to study the failure modes of these beams. The experimental results are considered to be very reliable, so the beams almost become a benchmark for testing of analytical and numerical formulations. Two of these beams with different layouts XOB-1 and XB-1 are analysed using the computer program SEGNID. The two beams are simply supported reinforced concrete beams of 12 ft (365.76 cm) span length, with cross sectional dimension 27.75 x 9 in (70.5 x 22.86 cm), (see Fig. 6). The beams are subjected to central concentrated load until achieving the failure load. The

reinforcement and failure loads are shown in Table 1. The beam XOB-1 is also analysed by [KOMPFNER 83] and [CERVERA/HINTON 86] with layered plate elements for their study of the three dimensional nonlinear analysis of reinforced concrete plates and shells.

Taking advantage of symmetry, only one half of the beam with different mesh idealisation is considered mesh (A)-(D) (see Fig. 7) .
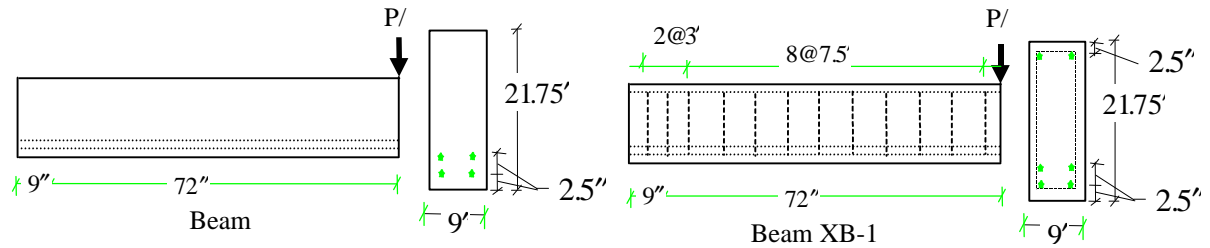
Figure 6 XOB-1 and XB-1 Beams Layout

Table 1. Reinforcement in the two Beams

Properties	XOB1	XB-1
Bottom Reinf.	4 #9	4 #9= 4 in^2
Top Reinf.	--	2 # 4 =0,372 in^2
Stirrups	--	# 2 - 7.5 in
Failure Load	57.5	90.0 kips

Table 2. The material used in analysis (ksi)

Properties	XOB-1 (kips)	XB-1 (kips)
Ec	3300	4120
fc	3.16	3.56
ft	Variable	0.572
ε_{cu}	0.003	variable
Es	27800	*
E$_H$	0	0
fy (Bottom)	90.6	90.6
fy (Top)	50.4	50.4

*Es = 27800, 28200 and 29500 for #9, # 4 and #2 respectively .

Table 3. Failure Load for XOB-1 Beam

f$_t$	Mesh A	Mesh B	Mesh C	Mesh D
0.333	58	56.5	58	56,5
0.565	62,7	60.5	62	60
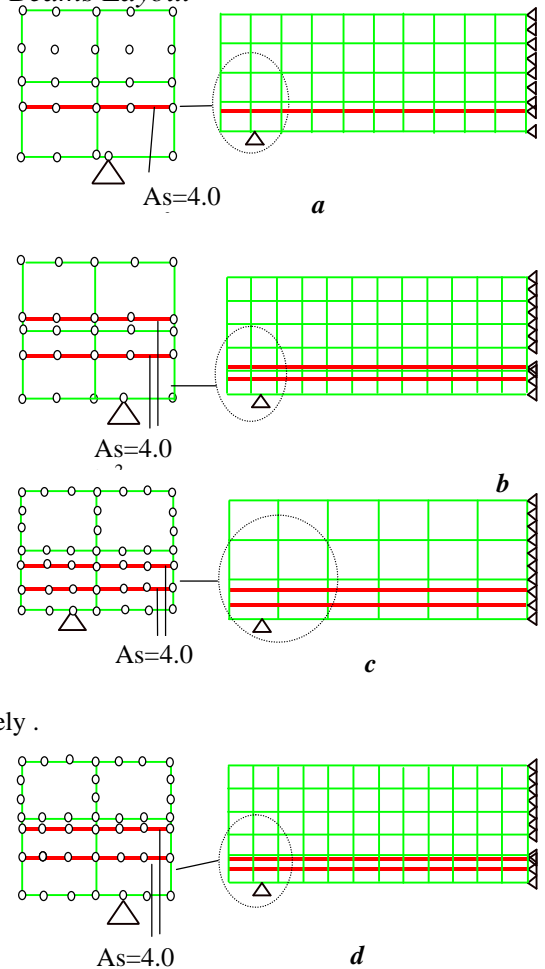
Figure 7 Finite Element Meshes for XOB-1 Beam

The experimental failure loads are reported to be 57.5 kips and 90.0 kips for XOB-1 and XB-1 beam respectively.

The value of the concrete tension strength is assumed variable. The iteration tolerance in analysis for all meshes is 0.1%. An elastoplastic concrete material model with quadratic hardening function developed by [DINGES 87] was used. The effect of the tension stiffening parameter will be not discussed here. The failure load is calculated using the different meshes and different concrete tension strengths (Table 3).

Figure 8 shows the load displacement curve compared with the experimental values using mesh C and different value of concrete tension strength.

Figure 8 Mid-Span Load Displacement Diagram

Figure 9 Effect of the C_{rr} on the Steel Stress
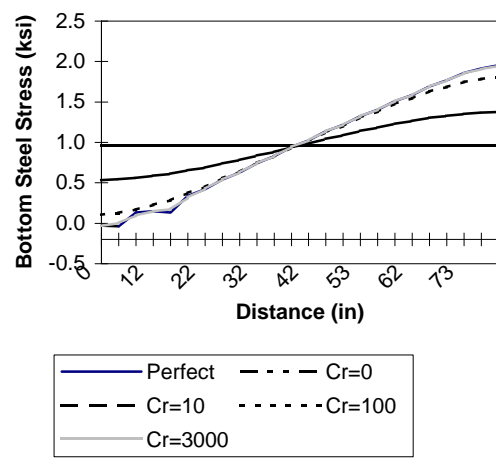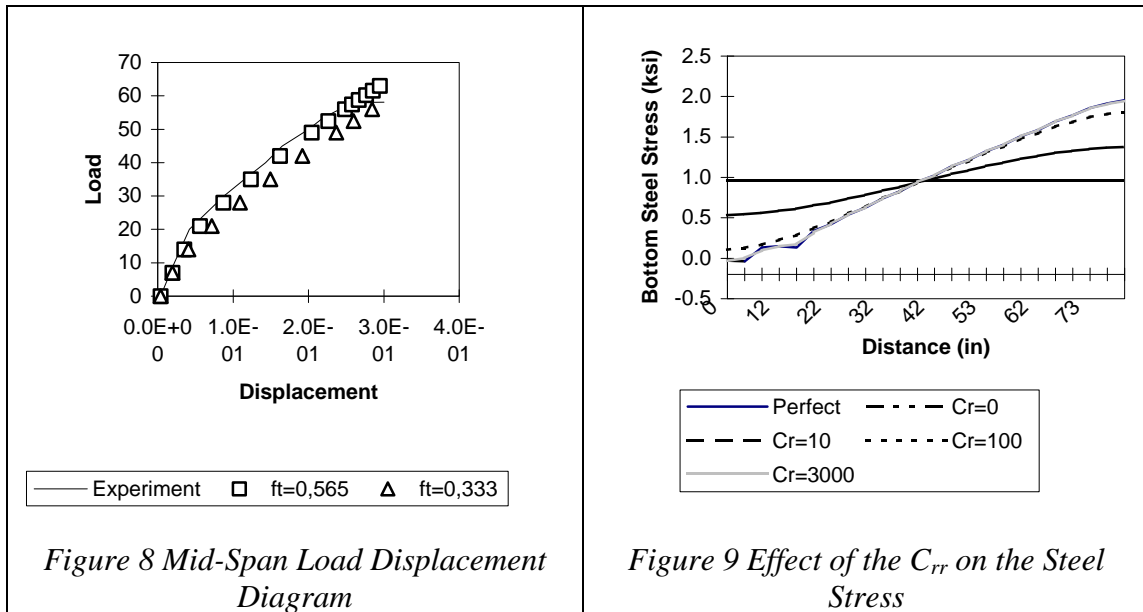
To see the effect of the bond model a simple bond model was used to consider the bond between steel and concrete. It is assumed that C_{rr} (The modulus of Elasticity of the contact element) is constant until Δ_r achieves the limit value Δ_1. Then the C_{rr} are set to equal zero.

Using Mesh B the effect of the value of C_{rr} on the bottom steel stress at P = 7 kips is shown in figure 9, where at this load stage there is no crack in concrete. The end nodes of the steel are assumed to be fixed to the concrete node. The relative displacements normal to the steel elements are disregarded. The effect of no bond is represented when C_{rr} =0. It is obvious that when there is no bond the steel stress is constant, but when the two ends are free, the steel stress is practically zero. With a high value of C_{rr} the steel stress is almost identical to a perfect bond.

The failure mode of beam XOB-1 is a diagonal-tension failure (D-T). The Crack progress at the Gauss points at the load case P=14 and 56 kips. is shown in Figure 10.

a   *b*
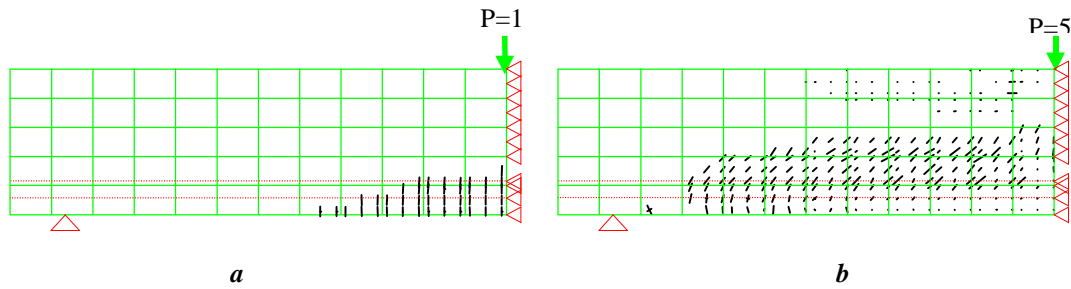
Figure 10 Cracks Propagation of the XOB-1 Beam

The Beam XB-1 has a shear compression failure (V-C). So the value of the ultimate concrete compressive strain has an important effect on the failure load in the analysis. Mesh B was considered in the analysis of XB-1 beam. The stirrups are represented by a smeared model and the main reinforcement by a discrete model (see Fig. 10). The failure load reported in the experiment was 90 kips. The effects of the ultimate concrete compressive strain (ε_{cu}) on the failure load are shown in Table 4. A very good agreement with the experimental result was achieved using ε_{cu} values between 0.0035 to 0.004.

Table 4. Effect of the Ultimate Compressive Strain

ε_{cu}	0.0025	0.003	0.0035	0.004
Pu (kips)	70	77	86	91
Error(%)	22.2	14.4	4.4	1.1

Stirrups as
Smeared model

As=4.0
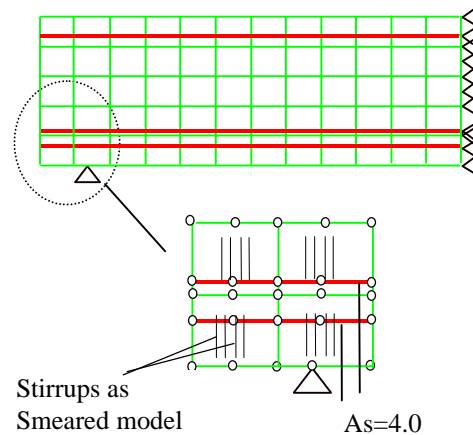
Figure 11 F.E. Mesh of XB-1 Beam.

7. REFERENCES

Bresler, B. & Scordelis, A. 1964. Shear Strength of Reinforced Concrete Beams-Series II. *Report No. 64-2, Structural Engineering Laboratory,* University of California, Berkeley, USA.

Cela, M. & Gray, W. 1984. An Improved Isoparametric Transformation for Finite Element Analysis. *Int. J. Num. Meth. Engng.* 20: 1443-1459

Cevera, M. & Hinton E. 1986. Nonlinear Analysis of Reinforced Concrete Plates and Shells using a Three Dimensional Model. *Computational Modelling of Reinforced Concrete Structures* by Hinton E. and Owen R., Pineridge Press Limited., 1986, Swansea, UK.

Citipitioglu, E. & Nicolas, V. 1979. Mapping Distortion in Parametric Finite Element Formulation and Mesh Generation. *Methodes Numeriques Dans Les Sciences de I'ingenieur,* Bordes, Paris

Dinges ,D. 1987 Vergleichende Untersuchungen von Stahlbetontragwerken unter Berücksichtigung physikalischer und geometrischer Nichtlinearitäten, Ph.D. Dissertation D17, TH Darmstadt.

El-Mezaini, N. & Citipitioglu, E. 1991. Finite Element Analysis of Prestressed and Reinforced Concrete structures. *Int. J. Struc. Engng.* 117(No. 10): 2851-2864.

Hofstetter, G. & Mang H., Computational Mechanics of Reinforced Concrete structures, F. Vieweg & Sohn, Braunschweig/Wiesbaden 1995

Keuser, M. & Mehlhorn, G. 1987. Finite Element Models for Bond problems. *J. Struc. Engng.* 113 (No. 10): 2160-2173.

Kompfner, T. 1983. Ein finites Elementmodell für die geometrisch und physikalisch nichtlineare Berechnung von Stahlbetonschalen. *Ph.D. Dissertation* at University of Stuttgart, Germany.(in German).

Ngo, D. & Scordelis, A. 1967. Finite Element Analysis of Reinforced Concrete Beam. *ACI J.* 64(No. 3): 152-163.